Astron. Astrophys. 319, 729–736 (1997)

ASTRONOMY
AND
ASTROPHYSICS

The anisotropy of the cosmic background radiation due to mass clustering in a closed universe⋆

Daming Chen[1], **Guoxuan Song**[1], **and Yougen Shen**[2,1]

[1] Shanghai Observatory, Academia Sinica, Shanghai, 200030, China
[2] China Center of Advanced Science and Technology (World Laboratory), P. O. Box 8730, Beijing 100080, China

Received 10 June 1996 / Accepted 11 September 1996

Abstract. We consider the effects on the Cosmic Background Radiation (CBR) of a single, spherically symmetric structure using the Tolman-Bondi solutions in a closed universe. The exact frequency shift of a photon passing through the center of a lump which is located between the last scattering surface and an observer is calculated. An approximate expression of the frequency shift $\frac{\Delta\nu_0}{\nu_0}$ to the first order of $\delta(x)$ (the density contrast) is given. We find that there are several redshifts of the perturbing lump where the net frequency shift is zero. With increasing Ω, the first positions of zero frequency shift move toward lower redshift; the larger the value of Ω, the further they move. At the vicinity of the last scattering surface, where the universe is close to flat, the frequency shift will always be the same as that for a flat universe.

Key words: cosmic microwave background – cosmology: theory – large-scale structure of the universe

1. Introduction

Since the COBE satellite discovered the anisotropy of the Cosmic Background Radiation (CBR) (Smoot et al. 1992; Bennett et al. 1992; Wright et al. 1992), a new era has been open in cosmology. As a matter of fact, soon after the discovery of the CBR, it was noted that the CBR temperature distortion would provide a sensitive probe of large-scale density inhomogeneities in the universe(Sachs & Wolfe,1967;Rees & Sciama,1968). Large-scale density perturbations in the universe will induce CBR anisotropy; the relationship between the anisotropy and the perturbation depends on how the inhomogeneity is produced. However, there has been a renewed interest in studying anisotropy of the CBR produced by the late time evolution of density inhomogeneities (Martinez-González & Sanz 1990; Martinez-González, Sanz, & Silk 1990, 1992; Panek 1992; Fang & Wu 1993; Meśzarós 1994; Meśzarós-González,Sanz, & silk 1994; Hu & Sugiyama 1994). Most of the studies considered the effects on the CBR of a single, spherically symmetric structure using a Swiss cheese model, thin-shell approximation, or the Tolman-Bondi solution (more e.g., Rees & Sciama 1968; Dyer 1976; Kaiser 1982; Thompson &Vishniac 1987; Dyer & Ip 1988; Nottale 1984). If the universe is homogeneous at last scattering, then gravitational field perturbations must subsequently grow from zero to their present value in order to account for the observed structure. This time-varying gravitational field will induce a CBR anisotropy which may not be very small compared with the anisotropy produced in the primordial instability condition(Jaffe, Stebbins & Frieman, 1994; Fang & Wu,1993). On the other hand, the CBR anisotropy depends primarily on the geometry of the universe, which in a matter- dominated universe is determined by Ω, and on the optical depth to the surface of last scattering. Therefore, the CBR anisotropy may also provide information on the value of Ω (Kamionkowski, Spergel & Sugiyama, 1994).

One of the most robust predictions of inflationary cosmology is that the universe after inflation becomes extremely flat, which corresponds to $\Omega = 1$. However, it is also possible to construct inflationary models with $\Omega > 1$ (Linde,1995). From observational cosmology we know that the density parameter of the universe has not been finally determined, the accepted range is believed to be $0.1 \sim 4.0$. Recently, White and Scott (1996) considered structure formation and CBR anisotropy in a closed universe, both with and without cosmological constant.

Fang and Wu (1993) studied in detail the CBR anisotropy due to spherical clustering located between the last scattering surface and the observer. They considered only the flat universe case($\Omega = 1$). In this paper, we shall investigate the anisotropy due to collapsing spherical clustering located from the last scattering surface to the observer in a closed universe ($\Omega > 1$). Like Kamionkowski et al., we are interested in the effect of Ω on CBR anisotropy. Although it is difficult to quantitatively determine the value of Ω with this method at present time, it can provide important information. Furthermore, if the CBR anisotropies

Send offprint requests to: Daming Chen

⋆ Supported by the National Natural Science Foundation of China and the Young Astronomer Laboratory of Shanghai Observatory

on all angular scales are mapped out with great precision, the method presented here can at least provide reference values of Ω to be checked by other ways.

In Sect. 2, we calculate in detail the linearized result of the CBR temperature distortion. The analytical solution is seemingly complex but actually clear.

In Sect. 3, the numerical result are given, and we discuss the results.

2. Temperature distortion

As shown by Fang and Wu (1993)(FW, hereafter), the metric for a spherically symmetric overdense perturbation in an expanding universe can be generally written as:

$$\mathrm{d}s^2 = e^{\lambda(x,t)}\mathrm{d}x^2 + r^2(x,t)(\mathrm{d}\theta^2 + \sin^2\theta\mathrm{d}\phi^2) - \mathrm{d}t^2. \tag{1}$$

Writing

$$r = S(x,t)x \tag{2}$$

and

$$S(x,t_i) = 1 \tag{3}$$

one can obtain the dynamical equation of $S(x,t)$ as

$$\dot{S}^2 - H_i^2\frac{\bar{\rho}(x,t_i)}{\rho_{ci}}\frac{1}{S} = H_i^2[1 - \frac{\bar{\rho}(x,t_i)}{\rho_{ci}}] \tag{4}$$

where $H_i = (\dot{S}/S)_{t=t_i}$ and $\rho_{ci} = 3H_i^2/8\pi$ are the Hubble parameter and critical density of the universe at $t = t_i$ (the decoupling epoch; for convenience, we assume in this paper that the decoupling epoch is at the same time when the last scattering takes place.), respectively.

$$\bar{\rho}(x,t_i) = \frac{\int_0^r \rho r^2\mathrm{d}r}{\int_0^r r^2\mathrm{d}r} \tag{5}$$

is the mean density within the shell of radius x.

As did FW, we consider an initial over-density perturbation region which is located at the origin($x = 0$) and at $t = t_i$:

$$\begin{cases}\rho(x,t_i) = \rho_i(1+\delta_0), & x \le x_0\\ \rho(x,t_i) = \rho_i, & x > x_0\end{cases} \tag{6}$$

then

$$\bar{\rho}(x,t_i) = \rho_i[1+\delta(x)] \tag{7}$$

where

$$\delta(x) = \begin{cases}\delta_0, & x \le x_0\\ \delta_0(x_0/x)^3, & x > x_0\end{cases} \tag{8}$$

Eq.(4) can be rewritten as

$$\dot{S}^2 = H_i^2\left\{\Omega_i[1+\delta(x)](\frac{1}{S} - 1) + 1\right\} \tag{9}$$

where $\Omega_i = \frac{\rho_i}{\rho_{ci}}$ is the density parameter of the universe at $t = t_i$.

The dynamical solution of Eq.(9) is

$$t + t_0(x) = \frac{\Omega_i[1+\delta(x)]}{2H_i[\Omega_i(1+\delta(x)) - 1]^{\frac{3}{2}}}(\eta - \sin\eta) \tag{10}$$

$$S = \frac{\Omega_i[1+\delta(x)]}{\Omega_i[1+\delta(x)] - 1}\cdot\frac{1-\cos\eta}{2} \tag{11}$$

where the integral constant $t_0(x)$ is

$$\frac{t_0(x)}{t_i} = \frac{\Omega_i[1+\delta(x)]}{2H_i[\Omega_i(1+\delta(x)) - 1]^{3/2}}(\eta_i - \sin\eta_i) - 1$$

When $t \le t_i$, $\delta(x) = 0$, one finds

$$t = \frac{\Omega_i}{2H_i(\Omega_i - 1)^{\frac{3}{2}}}(\eta - \sin\eta) \tag{12}$$

$$S_0(t) = \frac{\Omega_i}{\Omega_i - 1}\cdot\frac{1-\cos\eta}{2} \tag{13}$$

Setting $\eta = \eta_i$ when $t = t_i$ in Eqs.(11), (12) and (13), noting that $S(t_i) = 1$, we obtain

$$\cos\eta_i = \frac{2}{\Omega_i} - 1 \tag{14}$$

$$\sin\eta_i = \frac{2}{\Omega_i}\sqrt{\Omega_i - 1} \tag{15}$$

$$t_iH_i = \frac{\Omega_i}{2(\Omega_i - 1)^{\frac{3}{2}}}[\eta_i - \frac{2}{\Omega_i}\sqrt{\Omega_i - 1}] \tag{16}$$

In order to obtain numerical results of the CBR temperature distortion, one has to find a linear approximation solution of $S(x,t)$. We set

$$S(x,t) = S_0(t) + \delta(x)S_1(t) \tag{17}$$

From Eqs.(9) and (17) one has

$$\frac{\mathrm{d}S_1}{\mathrm{d}\eta} + \frac{1}{\sin\eta}S_1 =$$

$$\frac{1}{2}[\frac{\Omega_i}{\Omega_i - 1}\tan(\frac{\eta}{2}) - (\frac{\Omega_i}{\Omega_i - 1})^2\tan\frac{\eta}{2}\sin^2\frac{\eta}{2}] \tag{18}$$

The solution of Eq.(18) is

$$S_1 = [\frac{\Omega_i}{\Omega_i - 1} - (\frac{\Omega_i}{\Omega_i - 1})^2](1 - \frac{\eta}{2}/\tan\frac{\eta}{2})$$

$$+\frac{1}{4}(\frac{\Omega_i}{\Omega_i-1})^2(\eta-\sin\eta)/\tan\frac{\eta}{2}+C/\tan\frac{\eta}{2} \quad (19)$$

where

$$C=-\{[\frac{\Omega_i}{\Omega_i-1}-(\frac{\Omega_i}{\Omega_i-1})^2]$$
$$(1-\frac{\eta_i}{2}/\tan\frac{\eta_i}{2})\tan\frac{\eta_i}{2}+\frac{1}{4}(\frac{\Omega_i}{\Omega_i-1})^2(\eta_i-\sin\eta_i)\} \quad (20)$$

Considering the photons which pass through the center of the collapsing lump, the photon trajectory equation in the zero-order approximation is

$$\begin{aligned}\frac{\mathrm{d}x}{\mathrm{d}t} &= \pm e^{-\lambda(x,t)/2}\\ &= \pm\frac{1}{S_0(t)}\sqrt{1-x^2H_i^2(\Omega_i-1)}\end{aligned} \quad (21)$$

where the signs minus and plus describe a photon moving toward and going away from the center of the lump, respectively.

The solution of Eq.(21) can be read as

$$H_i\sqrt{\Omega_i-1}x=\pm\sin(\eta-\eta_m) \quad (22)$$

where η_m is the parameter corresponding to a photon that is passing through the center of a lump.

The solution of the zero component of the null geodesic equation gives (FW),

$$\begin{aligned}k^0 &\sim \exp(-\int\frac{1}{2}\dot{\lambda}e^{\lambda/2}\mathrm{d}x)\\ &= \exp[\int\frac{1}{2}\frac{\mathrm{d}\lambda(\eta)}{\mathrm{d}\eta}\mathrm{d}\eta]\end{aligned} \quad (23)$$

thus the comoving observed frequency ν_0 at time t_0 (the present time) is related to the frequency ν_i emitted at the last scattering surface by

$$\frac{\nu_i}{\nu_0}=\exp[\int_{\eta_i}^{\eta_0}\frac{1}{2}\frac{\mathrm{d}\lambda(\eta)}{\mathrm{d}\eta}\mathrm{d}\eta] \quad (24)$$

where the parameter η_0 is determined by the present time t_0.

The solution of Einstein equation gives

$$\frac{1}{2}\dot{\lambda}=\frac{\dot{r}'}{r'}=\frac{x\dot{S}'+\dot{S}}{xS'+S} \quad (25)$$

where the prime denotes derivative with respect to x.

In the case $\delta(x)=0$,

$$\frac{1}{2}\dot{\lambda}=\frac{\dot{S}_0}{S_0},$$

or

$$\frac{1}{2}\frac{\mathrm{d}\lambda}{\mathrm{d}\eta}=\frac{\mathrm{d}S_0}{\mathrm{d}\eta}\cdot\frac{1}{S_0} \quad (26)$$

From Eqs.(24) and (26), one obtains the 'position' of last scattering surface:

$$\begin{aligned}\frac{\nu_i}{\nu_0} &= \exp[\int_{\eta_i}^{\eta_0}\frac{\mathrm{d}S_0}{\mathrm{d}\eta}\cdot\frac{1}{S_0}\mathrm{d}\eta]\\ &= \frac{S_0(\eta_0)}{S_0(\eta_i)}\\ &= \frac{1-\cos\eta_0}{1-\cos\eta_i}\\ &= 1+z.\end{aligned} \quad (27)$$

Here $z=\frac{\nu_i-\nu_0}{\nu_0}$ is the redshift of a photon emitted from the last scattering surface, and ν_0 is the observed frequency of a photon in the unperturbed case.

If a photon passes through the center of a perturbing lump and is observed with the frequency ν_0, there is an extra frequency shift $\Delta\nu_0$ compared with photons in the unperturbed case. So we rewrite Eq.(27) as

$$1+z=\frac{\nu_i}{\nu_0-\Delta\nu_0}. \quad (28)$$

Eqs.(24) and (28) give the frequency shift

$$\frac{\Delta\nu_0}{\nu_0}=1-\frac{1}{1+z}\exp[\int_{\eta_i}^{\eta_0}\frac{1}{2}\frac{\mathrm{d}\lambda}{\mathrm{d}\eta}\mathrm{d}\eta] \quad (29)$$

In the first order approximation, by using Eqs.(17) and (19), one can find from Eq.(25) that

$$\frac{1}{2}\frac{\mathrm{d}\lambda}{\mathrm{d}\eta}=\frac{\sin\eta}{1-\cos\eta}$$
$$+\frac{1}{\frac{1-\cos\eta}{2}\frac{\Omega_i}{\Omega_i-1}}[x\delta'(x)+\delta(x)]\cdot(\frac{\mathrm{d}S_1}{\mathrm{d}\eta}-\frac{\sin\eta}{1-\cos\eta}S_1). \quad (30)$$

One thus has the expression of frequency shift to the first order of $\delta(x)$:

$$\frac{\Delta\nu_0}{\nu_0}=$$
$$-\int_{\eta_i}^{\eta_0}[x\delta'(x)+\delta(x)]\frac{1-\cos\eta}{2}\frac{\Omega_i-1}{\Omega_i}(\frac{\mathrm{d}S_1}{\mathrm{d}\eta}-\frac{\sin\eta}{1-\cos\eta})\mathrm{d}\eta. \quad (31)$$

3. Numerical results

From Eqs.(8),(19), (22) and (31), one can obtain an analytical result for the frequency shift, in the linearized approximation. However, there is a term $\int \ln(U + U_m)\mathrm{d}\eta$, where $U = \frac{1}{\tan\frac{\eta-\eta_m}{2}}, U_m = \frac{1}{\tan\frac{\eta_m}{2}}$, for which no analytical solution is available. One thus needs an expansion in series for the expression, which has different forms in three different regions. The results can be written as:

$$\frac{\Delta\nu_0}{\nu_0} =$$

$$\begin{cases} A_3(\eta_{c+},\eta_m) - A_3(\eta_0,\eta_m) \\ +A_2(\eta_i,\eta_m) - A_2(\eta_{c+},\eta_m), \\ (\text{for} \quad \eta_m < \sin^{-1}[X_c W_1\sqrt{\Omega_i - 1}]) \\ \\ A_1(\eta_{c-},\eta_m) - A_1(\eta_i,\eta_m) + A_1(\eta_{c+},\eta_m) - A_1(2\eta_m,\eta_m) \\ -A_3(\eta_0,\eta_m) + A_3(2\eta_m,\eta_m) + A_2(\eta_{c-},\eta_m) - A_2(\eta_{c+},\eta_m), \\ (\text{for} \quad \sin^{-1}[X_c W_1\sqrt{\Omega_i - 1}] < \eta_m < \frac{\eta_0}{2}) \\ \\ A_1(\eta_{c+},\eta_m) - A_1(\eta_0,\eta_m) + A_1(\eta_{c-},\eta_m) - A_1(\eta_i,\eta_m) \\ +A_2(\eta_{c-},\eta_m) - A_2(\eta_{c+},\eta_m), \\ (\text{for} \quad \frac{\eta_0}{2} < \eta_m < \eta_0) \end{cases} \quad (32)$$

where

$$\eta_m = \cos^{-1}[1 - \frac{1+z}{1+z_m}\cdot\frac{2(\Omega_i-1)}{\Omega_i}] \quad (33)$$

$$\eta_{c-} = \eta_m - \sin^{-1}[X_c W_1\sqrt{\Omega_i - 1}] \quad (34)$$

$$\eta_{c+} = \eta_m + \sin^{-1}[X_c W_1\sqrt{\Omega_i - 1}] \quad (35)$$

$$\eta_0 = \cos^{-1}[1 - (1+z)\cdot\frac{2(\Omega_i-1)}{\Omega_i}] \quad (36)$$

$$W_1 = \frac{\Omega_i}{2(\Omega_i-1)^{3/2}}[\cos^{-1}(\frac{2}{\Omega_i} - 1) - \frac{2}{\Omega_i}\sqrt{\Omega_i - 1}] \quad (37)$$

$$X_c = \frac{x_0 H_i}{W_1} \quad (38)$$

The functions A_1, A_2 and A_3 are given in Appendix A. The parameters η_{c-} and η_{c+} denote, respectively, the times when the photons are just entering and leaving the collapsing lump.

It is not difficult to show that the relationship between the temperature distortion and the frequency shift is: $\frac{\Delta T}{T} = \frac{\Delta\nu_0}{\nu_0}$.

$\frac{\Delta T}{T} = \frac{\Delta\nu_0}{\nu_0}$ versus the different locations z_m for $\Omega_i = 1.000001(\Omega_0 = 1.001)$ is given in Fig. 1. From this plot we can see that for relatively small sizes of the perturbing lump there several positions z_m of the lump is located, for which the frequency shift is zero. When the position of the perturbing lump goes through one of these positions, the frequency shift changes its sign. Hereafter, these positions are called "zero positions".

For comparison, the frequency shift is derived also for a flat universe in Appendix B. It turns out that the temperature distortions as a function of the location of the clusterings are qualitatively similar to those in Fig. 1.

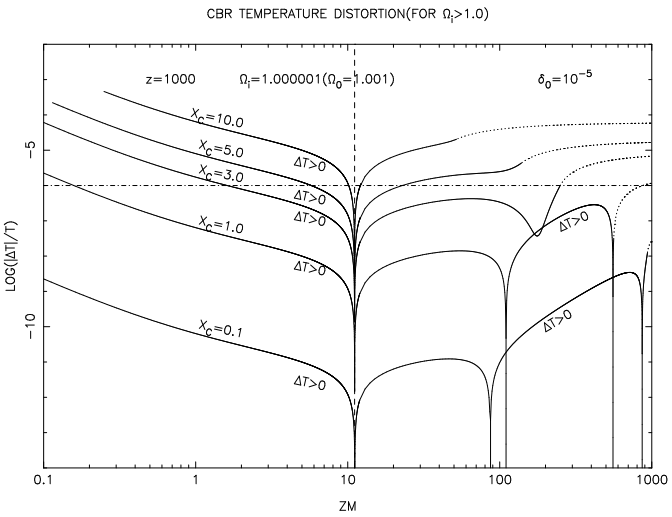

Fig. 1. CBR temperature distortion versus the location of a spherical clustering in an 'almost' flat universe, $\Omega_i = 1.000001$, corresponding to $\Omega_0 = 1.001$. $X_c = (H_i/W_1)x_0$ is a dimensionless quantity representing the size of the perturber, where H_i is the initial Hubble constant, W_1 is given in Eq.(37) depending on Ω_i and x_0 is the size of the perturber. For a small size of the perturber, there are several locations where zero CBR temperature distortion will arise. In this plot only positive temperature distortions are indicated.

By the way, it can easily find the difference between Fig. 1 in this paper and Fig. 1 in FW, where the same model as in this paper is adopted and the frequency shift $\frac{\Delta\nu_0}{\nu_0}$ to the first order is given by Eq.(32) in FW. In Eq.(32) of FW, three functions $G(T)$, $F_+(T)$ and $F_-(T)$ are included.

We recalculated the result $\frac{\Delta\nu_0}{\nu_0}$ for the flat universe from Eq.(28) in FW and found that $F_+(T)$ and $F_-(T)$ must be replaced by a single function $F(T)$, which could be read:

$$F(T) = F'(y) \quad (39)$$

$$F'(y) = \frac{y^2}{18a} - \frac{1}{9a^6}(-\frac{1}{3y^3} + \frac{5}{2y^2} - \frac{10}{y} - 10\ln|y| + 5y - \frac{y^2}{2}) \quad (40)$$

i.e., the only difference between Eq.(34) in FW and our Eq.(40) is the signs ' + ' and ' − ' before the term $\ln|y|$.

Eq.(32) in FW will be correctly rewritten as

$$\frac{\Delta\nu_0}{\nu_0} = -\frac{4}{15}\delta_0 X_c^3[F(T_0) + F(0) - F(T_{c-}) - F(T_{c+})] + \frac{2}{15}\delta_0[G(T_{c+}) - G(T_{c-})] \quad (41)$$

where $G(T)$ is as same as Eq.(37) in FW.

The detailed calculation is given in Appendix B.

Although it seems that the difference in the expression between FW and ours is tiny, the influence on the result is very important. As in a closed universe, in a flat universe there are

several zero positions when X_c is small enough (see Fig. 1). How to interpret the extra zero positions is one question, and whether or not there exist several zero positions is another. We adopt the interpretation given by FW for the first zero position, according to which, when a photon passes through a collapsing lump, the gravitational field is weaker for a photon travelling toward its center, which results in a positive shift of the CBR frequency, and stronger for a photon leaving from its center, which results in a negative shift of the CBR frequency. In a general way, therefore, the negative shift effect always wins out over the positive one except when the location of the collapsing lump is close enough to the observer. therefore, the net contribution of a collapsing lump to the frequency shift of the CBR is always negative except in a certain position, where the location of the lump is so close to the observer that there is only a part of the maximum negative effect of frequency shift that can cancel the positive one. That is to say, there must exist a location of the collapsing lump where the net contribution to the frequency shift of the CBR is zero. However, one can see from Fig. 1 that the number of positions of perturber (the collapsing lump) giving a zero frequency shift is either 1 or 3, which ensures that when the perburber is located near the last scattering surface, the temperature distortion (the frequency shift) is negative. Clearly, we can not interpret the extra zero positions with the same way that used to interpret the first zero positions, the detailed research on this problem will be given in a successive paper.

In order to investigate the influence of Ω_i on the CBR anisotropy, the CBR temperature distortion (anisotropy) as a function of the location of the collapsing lump is plotted in Fig. 2 for three different values of the density parameter of the universe. The values of these density parameters of the universe fall within the range accepted by current observational cosmology (i.e., $0.1 \leq \Omega_0 \leq 4.0$). Common characteristics in Fig. 2a, Fig. 2b and Fig. 2c are: (1) when X_c is large enough (in our model, when $X_c \geq 1.0$), the CBR anisotropy induced by a collapsing lump near the observer has the same order of magnitude as that near the last scattering surface, whereas with a smaller size of the lump (e.g., when $X_c \leq 0.1$), the CBR anisotropy near the observer is one order of magnitude less than that near the last scattering surface. (2) when the size of the lump is small enough (in our model, when $X_c \leq 1.0$), there exist more than one position where the CBR frequency shift induced by the lump located there is zero, and when z_m crosses a zero position, the sign of the CBR temperature distortion (i.e., the CBR anisotropy) changes. (3) The first zero positions will move to the left with increasing Ω_i, or with decreasing X_c for a fixed Ω_i. The larger the value of Ω_i or the smaller the size of the collapsing lump, the more the zero positions will move. On the contrary, no matter what the value of the density parameter is, the distribution of the CBR temperature distortion induced by the lump with different sizes remains almost unchanged near the last scattering surface, which, as a matter of fact, makes no difference with that in a flat universe. (4) In all the figures, the dotted lines denote the region that the collapsing lump situated there would cross with the last scattering surface. The connecting point of the two different style of lines corresponding to a certain value of X_c remains unchanged with the increasing values of Ω_i. In fact, the position of each connecting point in closed universes is just the same as that in a flat universe.

On the other hand, one can see clearly the difference of the influence on the CBR anisotropy due to the different values of the density parameter of the universe. As mentioned above, a connecting point is a critical position (which will be refered as 'critical position(s) 1', hereafter.) which determines whether the lump will cross the last scattering surface. There exist similar critical positions ('critical position(s) 2' hereafter.) near the observer which determine whether the observer is situated inside the lump. In our figures, the CBR temperature distortions induced by the lumps situated between the observer and the critical positions 2 are not plotted. In contrast to the fact that the critical position 1 corresponding to any definite size of a lump remains the same in closed universes determined by various values of Ω_i as well as in flat universe, critical positions 2 will move to the left with increasing Ω_i. When $\Omega_0 = 1.5$ or $\Omega_0 = 2.0$, as long as X_c is large enough (in our model when $X_c \geq 10.0$), one can find the critical position 2 in the range $0.1 \leq z_m \leq 1000.0$ (for which our results are plotted). As it does, in the universe defined by larger Ω (Ω_i or Ω_0), the distance between the observer and the center of a lump is larger, provided the redshift of the photons coming from the center of a lump is the same. This implies that the influence of the density parameter of the universe on CBR anisotropy varies with the evolution of the universe: it is stronger in late times than that in early times.

Compared with the case of a flat universe, when $\Omega_0 = 1.1$ each of the first zero positions corresponding to different sizes of the lump moves to the left, whereas the second zero positions corresponding to $X_c = 0.1$ and $X_c = 1.0$ respectively, move to the right (see Fig. 2a). When $\Omega_0 = 1.5$, each first zero position moves to the left as in the case $\Omega_0 = 1.1$, while the first zero position corresponding to $X_c = 0.1$ moves to the range of $0.1 \leq z_m \leq 1.0$; at the same time, each second zero position has moved further to the right compared with that in Fig. 2a (see Fig. 2b). When $\Omega_0 = 2.0$, each first zero position corresponding to $X_c = 0.1, 1.0, 3.0$ moves to the range $0.1 \leq z_m \leq 1.0$, while each second zero position is shifted further to the right (see Fig. 2c).

Actually, it is easy to show that if the universe is closed, in the decoupling epoch, one has:

$$\begin{aligned} \Omega_i - 1 &= \frac{\Omega_0 - 1}{1 + z\Omega_0} \\ &= \frac{1 - \frac{1}{\Omega_0}}{z + \frac{1}{\Omega_0}} \\ &< \frac{1}{z}. \end{aligned} \tag{42}$$

where Ω_0 is the present value of the density parameter of the universe. If $z \sim 10^3$, one finds that $(\Omega_i - 1)_{\text{uplimit}} \sim 10^{-3}$.

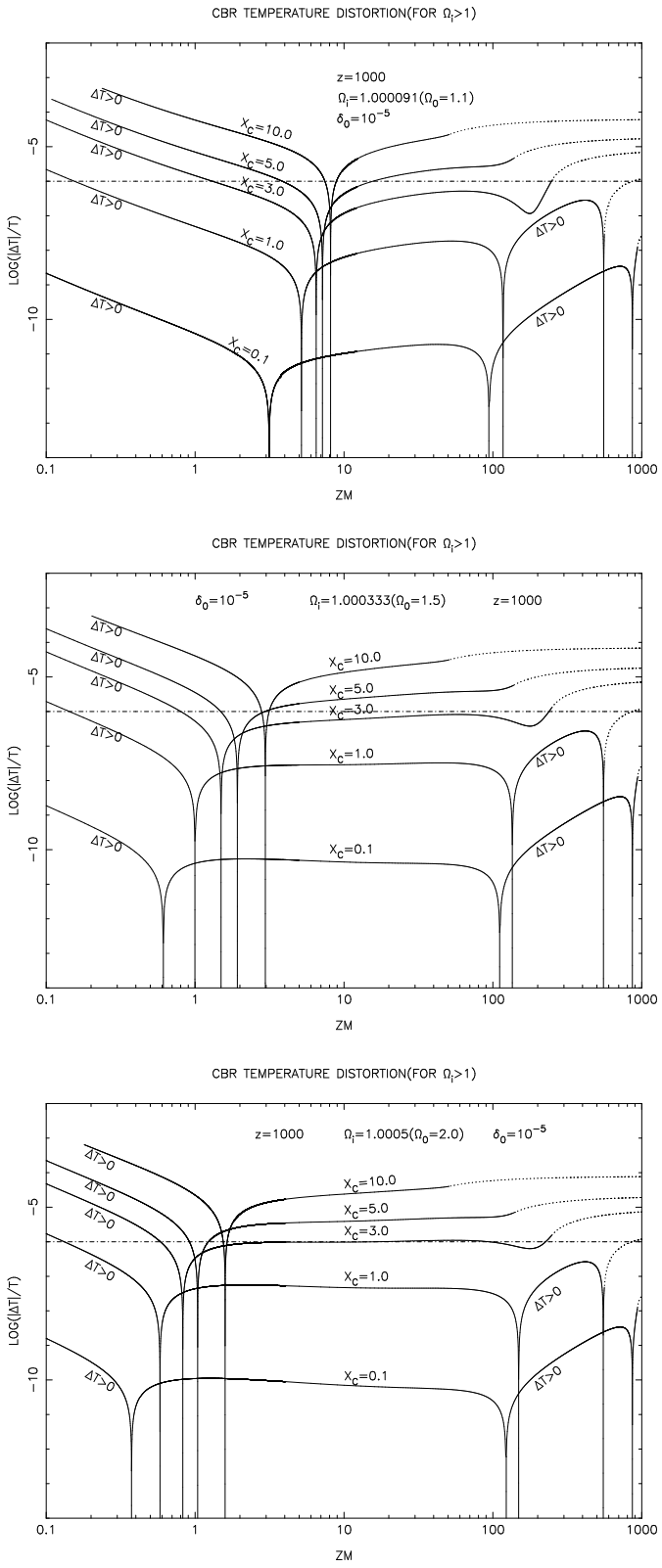

Fig. 2a–c. Same as Fig. 1, but with three larger values of Ω_i. The first zero positions move to the range of $0.1 \leq z_m \leq 1.0$ for smaller sizes of the perturber. **a** $\Omega_i = 1.000091$, $\Omega_0 = 1.1$ **b** $\Omega_i = 1.000333$, $\Omega_0 = 1.5$ **c** $\Omega_i = 1.0005$, $\Omega_0 = 2.0$

4. Conclusion and discussion

One can see from the numerical results that: (1) In a closed universe as well as in a flat universe, an initial perturbation located at the region $z_m < 10$ can cause an anisotropy as large as that caused by perturbations located on the last scattering surface; (2) near the observer, the density parameter plays a more important role than near the last scattering surface: e.g., when $z_m < 12$, with Ω increasing, the position of zero frequency shift moves toward lower redshifts, while the situation is almost unchanged in the region $z_m > 12$.

The appearance of extra zero positions of frequency shift may imply that the first order approximation for $\delta(x)$ is too crude, the method provided here can only describe the main characters of the frequency shift.

Appendix A

The functions in Eq.(32) are:

$$A_1(\eta,\eta_m) = -Q(P_1+F_1)$$
$$A_2(\eta,\eta_m) = \delta_0 S_1/\sin^2\tfrac{\eta}{2}$$
$$A_3(\eta,\eta_m) = -Q(P_2+F_1)$$

where

$$Q = 2(\Omega_i-1)^{3/2}\delta_0(X_cW_1)^3$$

$$F_1 = (\tfrac{\Omega_i-1}{\Omega_i})\tfrac{S_1}{\sin^3(\eta-\eta_m)\sin^2\frac{\eta}{2}}$$

$$P_1 = -6F_2-6W_2Z_1-3C'Z_2+F_3+F_4+\tfrac{3}{2}W_2(\eta Z_2-Z'_{22}-Z_3)$$

$$P_2 = -6F_2-6W_2Z_1-3C'Z_2+F_3+F_4+\tfrac{3}{2}W_2(\eta Z_2-Z'_{21}-Z_3)$$

$$W_2 = 1-\tfrac{3}{2}(\tfrac{\Omega_i}{\Omega_i-1})$$

$$C' = \tfrac{\Omega_i-1}{\Omega_i}\cdot C$$

$$F_2 = \tfrac{\cos(\eta-\eta_m)}{\sin^4(\eta-\eta_m)}[W_2/\tan\tfrac{\eta}{2}+\tfrac{C'}{2}/\tan^2\tfrac{\eta}{2}]$$

Setting $U = 1/\tan\frac{\eta-\eta_m}{2}$, $U_m = 1/\tan\frac{\eta_m}{2}$, we have:

$$Z_1 = -\tfrac{U_m}{4}(-\tfrac{1}{2U^2}-\tfrac{1}{4U^4}+\tfrac{1}{2}U^2+\tfrac{1}{4}U^4)+\tfrac{1+U_m^2}{4}\cdot\{(-\tfrac{3}{2U_m}$$
$$+\tfrac{U+U_m}{U_m^2})\tfrac{1}{U^2}+\tfrac{1}{U_m^3}\ln|\tfrac{U}{U+U_m}|+[-\tfrac{25}{12U_m}+\tfrac{13(U+U_m)}{3U_m^2}$$
$$-\tfrac{7(U+U_m)^2}{2U_m^3}+\tfrac{(U+U_m)^3}{U_m^4}]\tfrac{1}{U^4}+\tfrac{1}{U_m^5}\ln|\tfrac{+}{(}1+3U_m^2)U$$
$$-\tfrac{3}{2}U_m(U+U_m)^2UU+U_m|+\tfrac{1}{3}(U+U_m)^3$$
$$-(U_m+U_m^3)\ln|U+U_m|\}$$

$$
\begin{aligned}
Z_2 \;=\; & -\tfrac{(1+U_m^2)^2}{4}(\tfrac{1}{U_m^3}+\tfrac{5}{U_m^5})\tfrac{1}{U}+\tfrac{1}{8}(7+2U_m^2+\tfrac{11}{U_m^2}+\tfrac{5}{U_m^4})\tfrac{1}{U^2} \\
& -\tfrac{1+U_m^2}{12}(\tfrac{3}{U_m}+\tfrac{5}{U_m^3})\tfrac{1}{U^3}+(\tfrac{1}{2}+\tfrac{5}{16U_m^2}+\tfrac{1}{4}U_m^2)\tfrac{1}{U^4} \\
& +U_m(1+U_m^2)^2U-\tfrac{1}{8}(1+5U_m^2+3U_m^4)U^2+\tfrac{1}{6}U_m \\
& (1+U_m^2)U^3-\tfrac{U_m^2}{16}U^4-\tfrac{7}{12}U_m^4(1+U_m^2)-\tfrac{(1+U_m^2)^2}{4} \\
& (1+5U_m^2)\ln|U|+\tfrac{(1+U_m^2)^2}{4}(\tfrac{1}{U_m^4}+\tfrac{5}{U_m^6}-1-5U_m^2) \\
& \ln\left|1+\tfrac{U_m}{U}\right|-\tfrac{(1+U_m^2)^2}{4U_m}\tfrac{1}{(U+U_m)U^2}-\tfrac{(1+U_m^2)^2}{4U_m} \\
& \cdot\tfrac{1}{(U+U_m)U^4}-\tfrac{(1+U_m^2)^3U_m}{4}\cdot\tfrac{1}{U+U_m}
\end{aligned}
$$

We meet in the calculation a term $\int Z_2 \mathrm{d}\eta$, which can be expressed as

$$
\int Z_2 \mathrm{d}\eta = \begin{cases} Z'_{21}, & U < U_m \\ Z'_{22}, & U > U_m \end{cases}
$$

where in Z'_{21}, one has : $\ln(U+U_m) = \ln|U_m| + \frac{U}{U_m} - \frac{1}{2}(\frac{U}{U_m})^2 + \frac{1}{3}(\frac{U}{U_m})^3 - \frac{1}{4}(\frac{U}{U_m})^4$; in Z'_{22},

one has: $\ln(U+U_m) = \ln|u| + \frac{U_m}{U} - \frac{1}{2}(\frac{U_m}{U})^2 + \frac{1}{3}(\frac{U_m}{U})^3 - \frac{1}{4}(\frac{U_m}{U})^4$. One thus has

$$
\begin{aligned}
Z'_{21} \;=\; & \tfrac{(1+U_m^2)^2}{2}(\tfrac{1}{U_m^3}+\tfrac{5}{U_m^5})[\ln|U|-\tfrac{1}{2}\ln(1+U^2)] \\
& +\tfrac{1}{4}(7+2U_m^2+\tfrac{11}{U_m^2}+\tfrac{5}{U_m^4})\cdot(\tfrac{1}{U}+\tan^{-1}|U|) \\
& +\tfrac{1+U_m^2}{6}(\tfrac{3}{U_m}+\tfrac{5}{U_m^3})[-\tfrac{1}{2U^2}-\ln|U|+\tfrac{1}{2}\ln(1+U^2)] \\
& +(1+\tfrac{5}{8U_m^2}+\tfrac{1}{2}U_m^2)\cdot[\tfrac{1}{3U^3}+\tfrac{1}{U}-\tan^{-1}U] \\
& -U_m(1+U_m^2)^2\ln(1+U^2)+\tfrac{1}{4}(1+5U_m^2+3U_m^4) \\
& (U-\tan^{-1}U)-\tfrac{U_m(1+U_m^2)}{6}\cdot[U^2-\ln(1+U^2)] \\
& +\tfrac{U_m^2}{8}(\tfrac{1}{3}U^3-U+\tan^{-1}U)-\tfrac{7}{12}U_m^4(1+U_m^2)\eta \\
& +\tfrac{(1+U_m^2)^2}{4U_m^4}(1+\tfrac{5}{U_m^2})\cdot\{\eta\ln|\tfrac{\eta-\eta_m}{2}|-2[\eta+\eta_m \\
& \ln|\eta-\eta_m|]+\tfrac{1}{36}(\eta-\eta_m)^3+\tfrac{7}{90\times80}(\eta-\eta_m)^5\} \\
& +\tfrac{(1+U_m^2)^2}{2U_m}\{[-\tfrac{11}{6U_m}+\tfrac{5(U+U_m)}{2U_m^2}-\tfrac{(U+U_m)^2}{U_m^3}]\tfrac{1}{U^3}+\tfrac{1}{U_m^4} \\
& \ln|\tfrac{U}{U+U_m}|\}+\tfrac{U_m(1+U_m^2)^2}{2}[\ln|U+U_m|-\tfrac{1}{2}\ln(1+U^2) \\
& +U_m\tan^{-1}U]+\tfrac{(1+U_m^2)^2}{4}(\tfrac{1}{U_m^4}+\tfrac{5}{U_m^6}-1-5U_m^2) \\
& \{\eta\ln|U_m|-\tfrac{1}{U_m}\ln(1+U^2)+\tfrac{1}{U_m^2}(U-\tan^{-1}U) \\
& -\tfrac{2}{3U_m^3}[\tfrac{1}{2}U^2-\tfrac{1}{2}\ln(1+U^2)]+\tfrac{1}{2U_m^4}(\tfrac{U^3}{3}-U+\tan^{-1}U)\}
\end{aligned}
$$

$$
\begin{aligned}
Z'_{22} \;=\; & \tfrac{U_m(1+U_m^2)^2}{2}(1+5U_m^2)[\ln|U|-\tfrac{1}{2}\ln(1+U^2)] \\
& +\tfrac{1}{4}(2U_m^2+7U_m^4+11U_m^6+5U_m^8)\cdot(\tfrac{1}{U}+\tan^{-1}U) \\
& +\tfrac{1+U_m^2}{6}(-\tfrac{3}{U_m}-U_m+U_m^3+6U_m^5+5U_m^7)[-\tfrac{1}{2U^2} \\
& -\ln|U|+\tfrac{1}{2}\ln(1+U^2)]+\tfrac{1}{8}(3+3U_m^2-7U_m^6-11U_m^8) \\
& \cdot(-\tfrac{1}{3U^3}+\tfrac{1}{U}+\tan^{-1}U)-U_m(1+U_m^2)^2\ln(1+U^2) \\
& +\tfrac{1}{4}(1+5U_m^2+3U_m^4)\cdot(U-\tan^{-1}U)-\tfrac{U_m(1+U_m^2)}{6} \\
& [U^2-\ln(1+U^2)]+\tfrac{U_m^2}{8}(\tfrac{U^3}{3}-U+\tan^{-1}U) \\
& -\tfrac{7}{12}U_m^4(1+U_m^2)\eta+\tfrac{(1+U_m^2)^2}{4}(1+5U_m^2)\{\eta\ln|\tfrac{\eta-\eta_m}{2}| \\
& -2[\eta+\eta_m\cdot\ln|\eta-\eta_m|]+\tfrac{1}{36}(\eta-\eta_m)^3+\tfrac{7}{90\times80} \\
& (\eta-\eta_m)^5\}+\tfrac{(1+U_m^2)^2}{2}\cdot\{[-\tfrac{11}{6U_m}+\tfrac{5(U+U_m)}{2U_m^2} \\
& -\tfrac{(U+U_m)^2}{U_m^3}]\cdot\tfrac{1}{U^3}+\tfrac{1}{U_m^4}\ln|\tfrac{U}{U+U_m}|\}+\tfrac{(1+U_m^2)^2U_m}{2} \\
& [\ln|U+U_m|-\tfrac{1}{2}\ln(1+U^2)+U_m\tan^{-1}U]
\end{aligned}
$$

$$
\begin{aligned}
Z_3 \;=\; & -\tfrac{1}{8}[-\tfrac{1}{U_m(U+U_m)}+\tfrac{22}{3U_m^2}-\tfrac{10(U+U_m)}{U_m^3}+\tfrac{4(U+U_m)^2}{U_m^4}] \\
& \tfrac{1}{U^3}-\tfrac{4}{8U_m^5}\ln|\tfrac{U}{U+U_m}|-\tfrac{U_m}{4}\{-[-\tfrac{1}{U_m(U+U_m)}+\tfrac{9}{2U_m^2} \\
& -\tfrac{3(U+U_m)}{U_m^3}]\tfrac{1}{U^2}+\tfrac{3}{U_m^4}\ln|\tfrac{U}{U+U_m}|\}+\tfrac{1+U_m^2}{8}\{-[-\tfrac{1}{U_m(U+U_m)} \\
& +\tfrac{2}{U_m^2}]\tfrac{1}{U}-\tfrac{2}{U_m^3}\ln|\tfrac{U}{U+U_m}|\}-\tfrac{U_m}{4}[\tfrac{1}{U_m(U+U_m)}+\tfrac{1}{U_m^2} \\
& \ln|\tfrac{U}{U+U_m}|]+\tfrac{1}{8}\tfrac{1+U_m^2}{U+U_m}+\tfrac{U_m}{4}\ln|U+U_m|+\tfrac{1}{8}\tfrac{U_m^2+3U_m^4+U_m^6}{U+U_m} \\
& +\tfrac{1}{4}(U_m+4U_m^3+2U_m^5)\ln|U+U_m|-\tfrac{1}{8}(1+7U_m^2 \\
& +6U_m^4)U+\tfrac{1}{8}(U_m+2U_m^3)\cdot(U+U_m)^2-\tfrac{U_m^2}{24}(U+U_m)^3
\end{aligned}
$$

$$
F_3 \;=\; -\tfrac{1}{2}(\tfrac{\Omega_i}{\Omega_i-1})\tfrac{1}{\sin^3(\eta-\eta_m)}
$$

$$
F_4 \;=\; \tfrac{3}{2}W_2\tfrac{\eta\cos(\eta-\eta_m)}{\sin^4(\eta-\eta_m)\tan^2\frac{\eta}{2}}
$$

Appendix B

From Eq.(28) in FW, we have

$$
\frac{\Delta\nu_0}{\nu_0} = -\frac{2}{15}\int_0^{T_0}[x\delta'(x)+\delta(x)](-e^{2T/3}+e^{-T})dT, \qquad \text{(B1)}
$$

where

$$[x\delta'(x)+\delta(x)] = \begin{cases} \frac{-2\delta_0 X_c^3}{X^3}, & 0 \le T \le T_{c-} \\ \delta_0, & T_{c-} \le T \le T_{c+} \\ \frac{-2\delta_0 X_c^3}{X^3}, & T_{c+} \le T \le T_0 \end{cases} \quad \text{(B2)}$$

Eq.(B.1) should be divided into three parts

$$\begin{aligned} \frac{\Delta\nu_0}{\nu_0} &= -\frac{2}{15}\int_0^{T_{c-}} \frac{-2\delta_0 X_c^3}{X^3}(-e^{2T/3}+e^{-T})\mathrm{d}T \\ &\quad -\frac{2}{15}\int_{T_{c-}}^{T_{c+}} \delta_0(-e^{2T/3}+e^{-T})\mathrm{d}T \\ &\quad -\frac{2}{15}\int_{T_{c+}}^{T_0} \frac{-2\delta_0 X_c^3}{X^3}(-e^{2T/3}+e^{-T})\mathrm{d}T. \end{aligned} \quad \text{(B3)}$$

X and T has the relation as expressed in Eq.(29)(FW), which can be rewritten as

$$X = \begin{cases} -3(e^{T/3}+a), & 0 \le T \le T_{c-} \\ 3(e^{T/3}+a), & T_{c+} \le T \le T_0 \end{cases} \quad \text{(B4)}$$

where $a = -exp\frac{Tm}{3}$ (From Eq.(36) in FW). thus

$$\begin{aligned} \frac{\Delta\nu_0}{\nu_0} &= -\frac{4}{15\times 27}\delta_0 X_c^3 \int_0^{T_{c-}} \frac{-e^{2T/3}+e^{-T}}{(e^{T/3}+a)^3}\mathrm{d}T \\ &\quad -\frac{2}{15}\delta_0 \int_{T_{c-}}^{T_{c+}} (-e^{2T/3}+e^{-T})\mathrm{d}T \\ &\quad +\frac{4}{15\times 27}\delta_0 X_c^3 \int_{T_{c+}}^{T_0} \frac{-e^{2T/3}+e^{-T}}{(e^{T/3}+a)^3}\mathrm{d}T \\ &= -\frac{4}{15\times 27}\delta_0 X_c^3 \int_0^{T_{c-}} [-K_1(T)]\mathrm{d}T \\ &\quad -\frac{2}{15}\delta_0 \int_{T_{c-}}^{T_{c+}} K_2(T)\mathrm{d}T \\ &\quad +\frac{4}{15\times 27}\delta_0 X_c^3 \int_{T_{c+}}^{T_0} [-K_1(T)]\mathrm{d}T \\ &= -\frac{4}{15}\delta_0 X_c^3[-\frac{1}{27}\int_0^{T_{c-}} K_1(T)\mathrm{d}T \\ &\quad +\frac{1}{27}\int_{T_{c+}}^{T0} K_1(T)\mathrm{d}T] + \frac{2}{15}\delta_0[-\int_{T_{c-}}^{T_{c+}} K_2(T)\mathrm{d}T] \end{aligned} \quad \text{(B5)}$$

where

$$\begin{aligned} K_1(T) &= \frac{e^{2T/3}-e^{-T}}{(e^{T/3}+a)^3}, \\ K_2(T) &= -e^{2T/3}+e^{-T}. \end{aligned} \quad \text{(B6)}$$

From Eqs.(B.5) and (B.6), it can be clearly found that there is only one function $F(T)$ other than the two functions $F_{\pm}(T)$, and that the symbol before the term $\ln|y|$ should be unique.

Let

$$\begin{aligned} F(T) &= \frac{1}{27}\int K_1(T)\mathrm{d}T, \\ G(T) &= -\int K_2(T)\mathrm{d}T. \end{aligned} \quad \text{(B7)}$$

then

$$\begin{aligned} F(T) &= F'(y), \\ y &= \frac{e^{T/3}}{e^{T/3}+a}. \end{aligned} \quad \text{(B8)}$$

$$\begin{aligned} F'(y) &= \frac{1}{27}\int \frac{e^{2T/3}-e^{-T}}{(e^{T/3}+a)^3}\mathrm{d}T \\ &= \frac{1}{27}\int \frac{e^{2T/3}}{(e^{T/3}+a)^3}\mathrm{d}T - \frac{1}{27}\int \frac{e^{-T}}{(e^{T/3}+a)^3}\mathrm{d}T \\ &= \frac{1}{9a}\int y\mathrm{d}y - \frac{1}{9a^6}\int \frac{(1-y)^5}{y^4}\mathrm{d}y \\ &= \frac{1}{18a}y^2 - \frac{1}{9a^6}(-\frac{1}{3y^3}+\frac{5}{2y^2} \\ &\quad -\frac{10}{y} - 10\ln|y| + 5y - \frac{y^2}{2}) \end{aligned} \quad \text{(B9)}$$

G(T) given by Eq.(B.7) is as the same as that in FW. Finally, from Eqs.(B.5), (B.6)and (B.7) one can obtain eq.(41) in this paper:

$$\begin{aligned} \frac{\Delta\nu_0}{\nu_0} &= -\frac{4}{15}\delta_0 X_c^3[F(T_0)+F(0)-F(T_{c-})-F(T_{c+})] \\ &\quad +\frac{2}{15}\delta_0[G(T_{c+})-G(T_{c-})] \end{aligned}$$

References

Bennett C. L. et al., 1992, ApJ 396, L7
Dyer C. C.,1976, MNRAS 175, 429
Dyer C. C. & Ip P. S. S., 1988, MNRAS 235, 895
Fang L. Z. and Wu X. P., 1993, ApJ 408, 25 (FW)
Hu W., & Sugiyama N. 1994, Phys. Rev. D 50, 627
Jaffe A. H., Stebbins A. & Frieman J. A., 1994, ApJ 420, 9
Kamionkowski M., Spergel D. & Sugiyama N., 1994, ApJ 426, L57
Kaiser N.,1982, MNRAS 198, 1033
Linde A., 1995, Phys. Lett. B 351, 99
Linde A., 1995, Phys. Rev. D 52, 6789
Martinez-González E., & Sanz J. L. 1990, MNRAS 247, 473
Martinez-González E., Sanz J. L., & Silk J., 1990, ApJ 355, L5
Martinez-González E., Sanz J. L., & Silk J., 1992, Phys. Rev. D 46, 4196
Martinez-González E., Sanz J. L., & Silk J., 1994, ApJ 436, L1
Meszárós A., 1994, ApJ 423, 19
Nottale L., 1984, MNRAS 206, 713
Panek M., 1992, ApJ 388, 225
Rees M.,& Sciama D., 1968, Nature 217, 511
Sachs R. G., & Wolfe A. M., 1967, ApJ 147, 73
Smoot G. F. et al., 1992, ApJ]396, L1
Thompson K. L., & Vishniac E. T., 1987, ApJ 313, 517
White M., & Scott D., 1996, ApJ 459, 415
Wright E. L. et al., 1992, ApJ 396, L13